Compatibilization of Semicrystalline Polymeric Alloys Through Sepiolite Addition

CONSUELO R. HERRERO, ENRIQUE MORALES, and JOSE LUIS ACOSTA*

Instituto de Ciencia y Tecnología de Polímeros, C.S.I.C., % Juan de la Cierva, 3 28006 Madrid, Spain

SYNOPSIS

This study was conducted to examine the possibilities offered by sepiolite as a compatibilizing agent in the incompatible blend consisting of poly(vinylidene fluoride) and polystyrene. The effect of sepiolite on the crystalline microstructure and morphology was determined through isothermal crystallization and spherulite growth of the system under study. The effect of sepiolite on the compatibility of the system was also studied. The glass-transition temperature was determined, as well as the Flory–Huggins thermodynamic interaction parameter through two different routes: differential scanning calorimetry and inverse gas chromatography. A parallel study was conducted for the compatible system poly(vinylidene fluoride)/poly(methyl methacrylate). © 1994 John Wiley & Sons, Inc.

INTRODUCTION

Pyro-piezoelectric materials are presently gaining increasing importance in the field of physical sensors because they are capable of transforming mechanical stress into electrical responses and vice versa.[1] As a general rule most of these materials are inorganic, which is the reason why practical applications present several inconveniences derived from intrinsic properties, such as hardness and stiffness. In addition these materials are expensive and difficult to obtain. To obviate these drawbacks research was conducted quite some time ago on polymeric materials with pyro-piezoelectric characteristics that were easy to process and inexpensive while at the same time showed good mechanical properties. These studies resulted in the development of several materials, among which poly(vinylidene fluoride) (PVF_2) and some of its blends and copolymers have been specially highlighted.[2] Thus a new approach was initiated to improve the pyroelectric and/or the mechanical properties of PVF_2 and its blends through the synthesis of new blends with several polymers. This route, however, presents serious inconveniences as a consequence of the low compatibility of PVF_2 in relation to most of the other polymers, which translates into a significant loss of its electrical properties due to the difficulty or impossibility for multiphasic materials to transport electric charge. This is the reason why the development of new pyro-piezoelectric materials from PVF_2 blends requires a previous compatibilization process in the majority of cases, which may be implemented following different methods,[3] one of which, compatibilization through finely ground inorganic fillers,[4–8] is the method of choice in this research.

Hence it is the main objective of this work to study the effect exerted by sepiolite both on the compatibility and the microstructure of an incompatible system, such as PVF_2/polystyrene (PS). A parallel study was conducted on the system PVF_2/poly(methyl methacrylate) (PMMA) to compare the results obtained with either system.

EXPERIMENTAL

The starting materials were PVF_2, kynar 720 supplied by Penwalt Corp. (U.K.); PMMA supplied by Repsol S.A.; PS, BASF product 143E; and sepiolite (SEP) PANSIL S.A. supplied by Tolsa S.A. SEP is a hydrated magnesium silicate with a specific surface (BET) of 240 m^2/g, Bet constant 323, Dubinin micropore volume 9.44 cm^3/g, and particle diameter

* To whom correspondence should be addressed.

Journal of Applied Polymer Science, Vol. 51, 1189–1197 (1994)
 CCC 0021-8995/94/071189-09

at 50% 7.34 μm. The binary blends as well as those containing SEP were prepared in a Brabender type torque rheometer, using a thermoplastic mixing chamber type W60 preheated to 473 K. Rotor speed was set at 60 rpm; 10 min of mixing were enough to generate a steady-state response, indicating uniform dispersion of the components.

Isothermal crystallization and melting were measured with a Perkin–Elmer differential scanning calorimeter, type DSC-7. The samples were heated to 220°C at which temperature they were maintained for 10 min in order to destroy their thermal history, and then they were rapidly cooled to their crystallization temperature, T_c, at a rate of 350°C/min. Finally melting was recorded at a heating rate of 5°C/min.

The glass-transition temperature, T_g, and nonisothermal crystallization were determined with a Mettler differential scanning calorimeter, type TA 4000. The samples were held at 220°C for 10 min and rapidly cooled to −100°C, their thermograms being recorded at a rate of 10°C/min.

Spherulite growth was followed over a Jenaval light microscope coupled to a Hot Stage Mettler FP82. The samples were maintained in the molten state at 220°C for 10 min and then rapidly cooled to the prefixed crystallization temperature, where the measurements were recorded.

The mechanodynamic tests were conducted in a Metravib viscoelasticimeter applying the forced vibration technique under stress-compression.

RESULTS AND DISCUSSION

Effect of SEP on Microstructure and Morphology of PVF_2/PS and PVF_2/PMMA Systems

One of the currently widely used approaches in the determination of the microstructure of semicrystalline polymers is the study of their crystallization kinetics considering that the kinetic parameters to be determined are closely related to the microstructure of the material. In case the material under study is a polymeric blend, the resulting microstructure will be both a function of the underlying polymer types and their thermodynamic compatibility. If one of the polymers is of a semicrystalline type, the kinetic parameters obtained from the kinetic crystallization study will be influenced by the nature of the polymers and the degree of their compatibility.[9,10] The problem becomes even more complex when a finely ground filler is incorporated into the blend (such as SEP in our case). This filler may prove to be active or inactive in the crystallization process.

To analyze such complex behaviour, an overall isothermal crystallization study was carried out, based on Avrami's equation[11]:

$$X(t) = 1 - \exp(-Kt^n) \qquad (1)$$

where $X(t)$ is the weight fraction of material crystallized at time t, K is the overall kinetic rate constant, and n is the Avrami exponent dependent on the type of nucleation and on the geometry of growing crystals. The values of n and K were obtained for each crystallization temperature from the graphic plot of $\log\{-\ln[1 - X(t)]\}$ versus $\log t$.

In order to simplify the study the isothermal kinetics of the systems under study[12] was examined for three compositions and one crystallization temperature, that is, the samples PVF_2/PMMA (90/10), PVF_2/PS (90/10), and PVF_2 (95/5). The other compositions, crystallized at other temperatures, agree with the conclusions reached in the discussion below.

Figure 1 shows the effect produced by PMMA and PS on the kinetic rate constant of PVF_2 in the presence or absence of SEP. It was observed that in the absence of SEP the kinetic rate constant of PVF_2 increases with increasing the PMMA concentration in the blend, yet diminishes at higher PMMA concentrations. In contrast, when SEP is present, the crystallization rate constant consistently diminishes as a function of increasing PMMA concentration. In the case of PS the opposite occurs: in the absence of SEP the crystallization rate constant diminishes, yet increases for high PS content. In the presence of SEP, however, the overall crystallization rate constant increases proportionately to a PS content increase.

When studying the effect of SEP on the PVF_2 crystallization rate constant, in its pure form as well as in its respective blends (Fig. 2), it can be seen that SEP acts in the same way as PMMA: at low

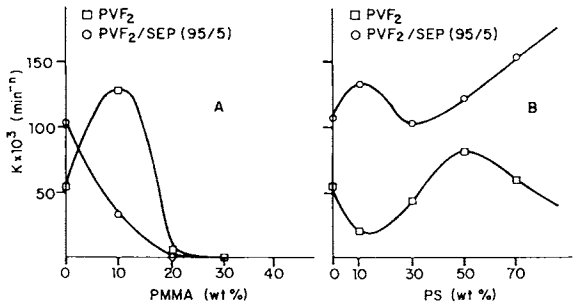

Figure 1 Effect of the PMMA or PS content on the isothermal overall kinetic rate constant K of the systems crystallized at 453 K.

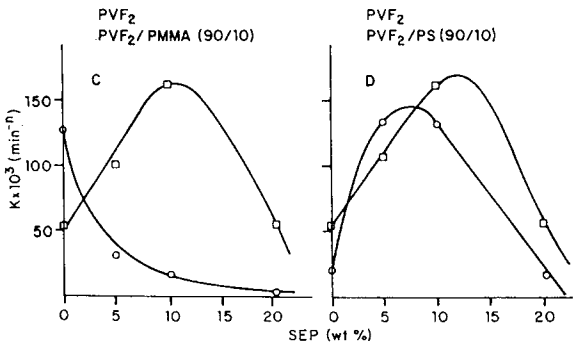

Figure 2 Effect of the SEP content on the isothermal overall kinetic rate constant K of the systems crystallized at 453 K.

SEP portions the crystallization rate constant of PVF_2 increases, but begins to diminish continuously with medium SEP concentrations. The rate constant shows the same behaviour, when SEP is incorporated into the PVF_2/PS system. In the PVF_2/PMMA system, however, SEP incorporation causes the rate constant to diminish inversely proportionate to SEP concentration.

This behaviour can be explained in terms of double action exerted by SEP. On the one hand it acts as a nucleating agent, and on the other it has a compatibility effect. The presence of SEP in the PVF_2/PMMA system would then be expected to increase the PVF_2 crystallization rate constant proportionate to increasing the SEP portion, as a function of its nucleating nature. The failure of this effect to occur is interpreted as a loss or masking of the surface activity of SEP as a consequence of specific interactions taking place between the filler and the polymeric system. The effect of SEP on the PVF_2/PS system can be interpreted in terms of the same criteria.

Regarding the growth geometry of the different systems, it is safe to assume it is independent of T_c, as well as being independent of the PMMA, PS, and SEP concentrations (Fig. 3) demonstrated by the practically constant values of Avrami's exponent n.

To study the nucleating and compatibilizing character of SEP in the isothermal crystallization of PVF_2 and/or its blends, spherulite growth of the PVF_2 portion in the different systems was examined. Insight into the effects produced by the individual components on spherulite growth and the nucleation density of PVF_2 was gained in this study. In light of these data the nucleating and compatibilizing character of the components can be established.

The spherulite growth rate of any crystalline polymer is governed by the Turnbull–Fisher equation[12] applicable to monoatomic substances:

$$G = G_0 \exp\left(\frac{-\Delta\phi^*}{kT_c}\right)\exp\left(\frac{-\Delta F^*}{kT_c}\right) \qquad (2)$$

where G_0 is a constant, T_c the crystallization temperature, and k the Boltzmann constant. $\Delta\phi^*$ represents the free energy required to form critical size nuclei from the melt. ΔF^* stands for the activation energy required to transport crystallizable units through the liquid–crystal interface.

When the crystalline polymer is in the molten state together with a second polymer acting as a diluant, the equation transcribed above adopts the following form:

$$\ln G - \ln \phi_2 + \frac{U^*}{R(T_c - T_\infty)} - \frac{0.2T_m \ln \phi_2}{\Delta T} = \ln G_0 - \frac{K_g}{T_c(\Delta T)f} \qquad (3)$$

where G_0 is the preexponential factor including the temperature independent factors, and $T_\infty = T_g - C$, C being a constant. f is a correction factor that takes into account the dependence of the thermodynamic heat of melting with the crystallization temperature[13] and is calculated by means of the expression $f = 2T_c/(T_m^\circ + T_c)$, T_m° being the equilibrium melting temperature of the semicrystalline polymer. U^* represents the sum of the activation energies for chain motion crystallizable and noncrystallizable molecules in the melt; K_g stands for the nucleation factor whose value is fundamentally related to the free energy necessary for the formation of the critical size nuclei.

The nucleation density, which determines the number of nuclei formed for each volume unit under

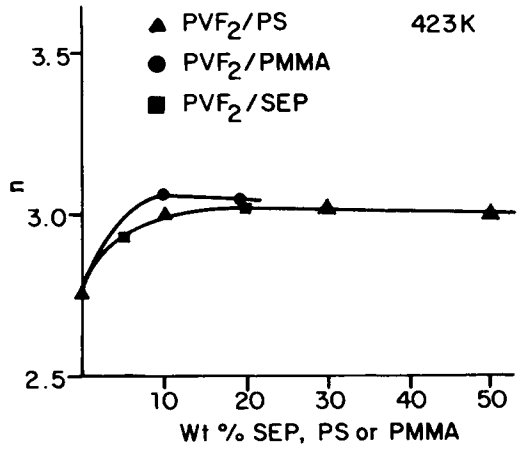

Figure 3 Effect of PMMA, PS, or SEP contents on the Avrami exponent n of the systems crystallized at 453 K.

the conditions imposed on the system, provides arguments in favour of or against the nucleating or inhibiting nature of the components. According to the general crystallization theory,[12] the nucleation density N, assuming the nucleation to be heterogeneous and the morphology to be spherulitic, satisfies the expression:

$$K_n = \frac{4}{3}\pi N G^3 \frac{\rho_c}{\rho_a}\frac{1}{1 - X_t} \qquad (4)$$

where G is the growth rate, K_n the crystallization rate constant, ρ_c and ρ_a stand for the densities of the crystalline and amorphous phases, respectively, X_t for conversion at infinite time. K_n is obtained from the expression,[14] $K_n = \ln 2/(t_{1/2})^n$, where $t_{1/2}$ is the isothermal crystallization halftime and n is Avrami's exponent.

The effect exerted by the presence of PMMA or PS on PVF_2 spherulite growth is represented in Figure 4. In the presence of PMMA, the spherulite growth rate diminishes inversely proportionate to the PMMA concentration, that is, it shows typical behaviour of compatible systems. In the case of PVF_2/PS blends the spherulite growth rate for each crystallization temperature is independent of PS concentration, which points toward the inmiscible nature of the system, the PVF_2 spherulites growing in their own melt without being affected by the presence of PS. When 5% SEP was incorporated into the PVF_2/PMMA system, SEP did not exert any effect whatsoever on PVF_2 spherulite growth.

The data obtained for nucleation density are compiled in Table I. SEP-free PVF_2 was proved to possess a lower nucleation density than the blend

Table I Nucleation Densities Values of Studied Blend at 428 K

Composition			$N\ 10^5$
PVF_2/PMMA	PVF_2/PS	SEP	(Nuclei/cm^3)
100/0	—	—	0.659
90/10	—	—	5.014
80/20	—	—	3.855
—	90/10	—	0.478
—	70/30	—	0.484
—	50/50	—	0.648
100/0	—	5	0.822
90/10	—	5	0.084
80/20	—	5	—

containing 5% SEP, which evidences SEP to be a nucleating agent. In the case of the PVF_2/PMMA system the opposite occurred: in the presence of SEP the nucleation density was lower than when absent from the blend, which is indicative of a specific interaction between SEP and PMMA or SEP selectively encapsulated in PMMA, which together inhibit the nucleating processes.

Effect of SEP on Compatibility of PVF_2/PS and PVF_2/PMMA Systems

In order to study the effect of SEP on the compatibility of compatible and incompatible PVF_2 blends, both the glass transitions and the Flory–Huggins interaction parameters of the different systems under study were determined.

The most widely used general criterion[3] to de-

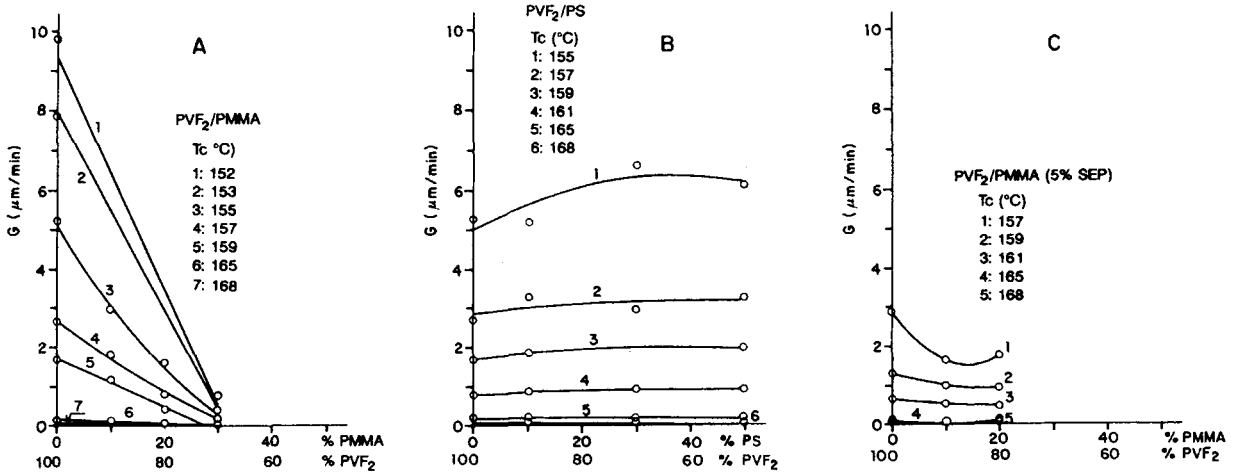

Figure 4 Variation of the spherulite growth rate with the composition for the crystallized temperatures examined.

termine the compatibility of a polymeric blend is that of the T_g, which obviates a blend of polymers to be compatible when it shows a single T_g intermediate between the values obtained for the individual components, the position of which on the scale varies as a function of blend composition. When a blend is totally incompatible two glass transitions are obtained, which coincide with those obtained for the individual unblended components. A blend is partially compatible, that is, there exists a certain degree of solubility of one polymer in the other, when two intermediate transitions are obtained within the temperature range between the T_gs of the individual components, which approach one another as a function of blend composition.

In the determination of the glass transitions for the different blends two distinct methods were employed: mechanical dynamic spectroscopy and differential scanning calorimetry (DSC).

The results obtained for the PVF_2/PMMA system with mechanical dynamic analysis [Fig. 5(A)], showed the glass transitions tend to converge with increasing PMMA content (independent of SEP content), which, according to the general criterion, is indicative of a partially compatible system. This seems to contradict in principle the specific literature on the subject,[13,15] where PVF_2/PMMA systems are defined as fully compatible over the whole compositional range.

As to the different PVF_2/PS compositions [Fig. 5(B)], the T_gs calculated by means of mechanical dynamic analysis remain practically unaltered when varying the PS portion in the blend. Neither does the presence or absence of SEP have any impact on this behaviour. This proves that we are dealing with an incompatible system and that SEP does not influence this situation according to the interpretation of the results obtained from mechanical dynamic analysis.

T_g determinations by DSC yielded partially contrary data to those obtained with the aforementioned technique. The results were analyzed by means of the models proposed by Gordon–Taylor[16] and Fox,[17] which are known to be models that describe the behaviour of compatible blends.

When DSC-analyzed, the PVF_2/PMMA blends and their SEP composites yielded one single glass transition each, whose value is a function of blends composition [Fig. 6(A)], the respective temperatures adjusting to the Gordon–Taylor model over the whole compositional range, as well as for all SEP portions incorporated. For the different PVF_2/PS blends and their SEP composites, when subjected to DSC two glass transitions were recorded that do not vary with blend composition or with SEP content [Fig. 6(B)]. The conclusions to be reached in the light of these results define the PVF_2/PMMA system as compatible with the whole compositional range, proved that SEP did not modify this behaviour, and showed the PVF_2/PS system to be totally incompatible, even in the presence of SEP.

Obviously these conclusions are not in agreement with those reached via mechanical dynamic analysis. This motivated the decision to use alternative routes to determine the compatibility of the systems under study, as well as the effect exerted by SEP on com-

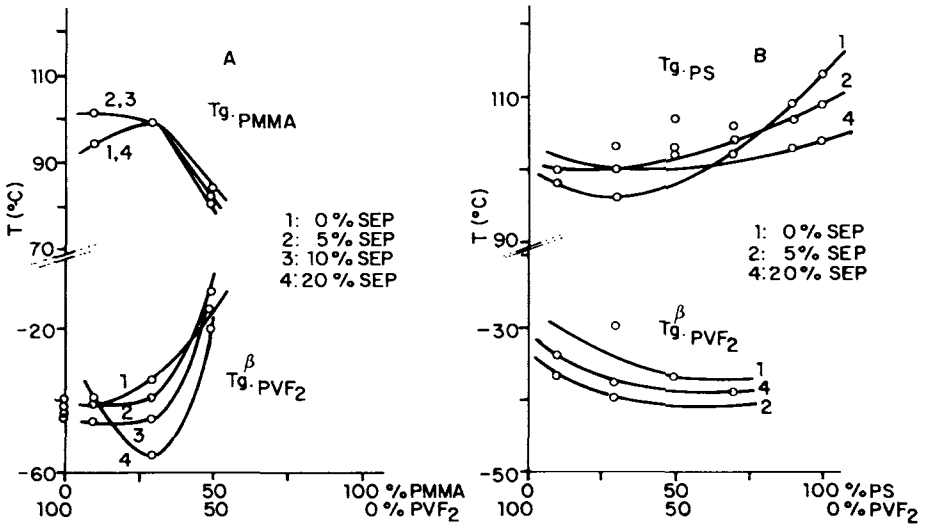

Figure 5 Effect of blend composition on the T_g of (A) PVF_2/PMMA and (B) PVF_2/PS blends at different loading of SEP.

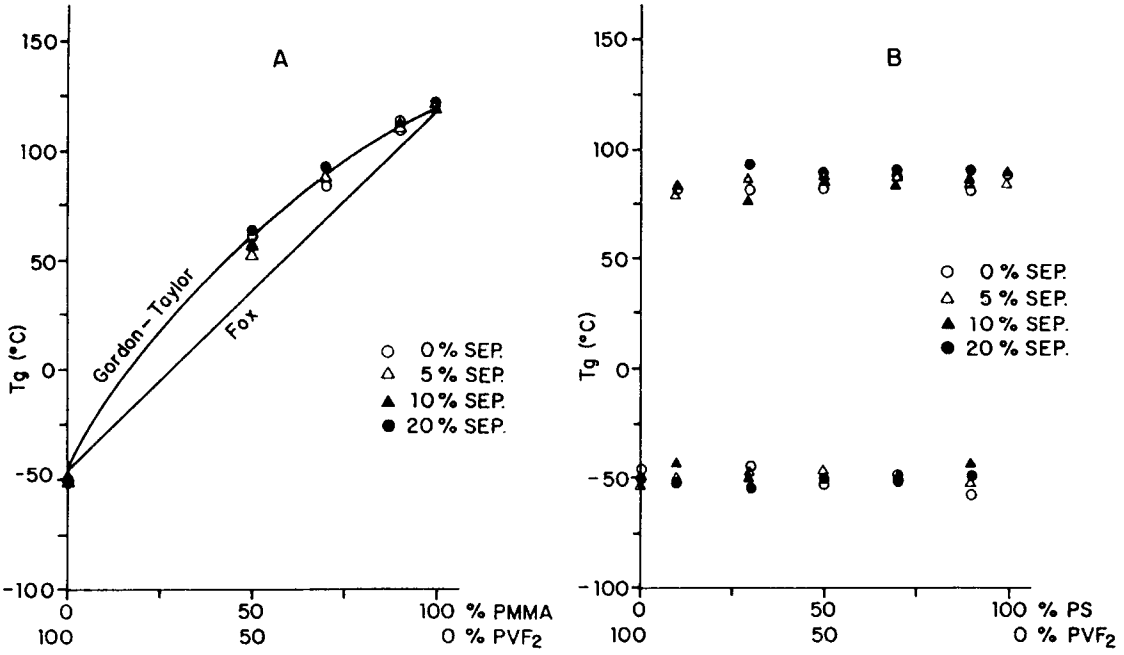

Figure 6 Effect of blend composition on the T_g of (A) PVF_2/PMMA and (B) PVF_2/PS blends at different loading of SEP.

patibility. One of the most commonly used approaches is the determination of the Flory–Huggins parameter, whose value and sign will permit the characterization of the systems from compatibility. Two types of analysis were used in parameter determination: the Nishi–Wang melting point depression[13] applicable to semicrystalline blends and inverse gas chromatography.

DSC allows the computation of the Flory–Huggins thermodynamic interaction parameter by means of the depression undergone by the melting point of semicrystalline polymer when in the presence of another polymer miscible with the former. The equation to determine the parameter was originally developed by Scott[18] and Koningsveld et al.[19] and subsequently optimized by Nishi–Wang[13]:

$$\frac{1}{T_m} - \frac{1}{T_m^\circ} = -\frac{RV_{2u}}{\Delta H_{2u} V_{1u}} X_{23} v_1^2 \qquad (5)$$

where the subindices 1 and 2 identify the amorphous and crystalline polymers, respectively, T_m° the thermodynamic melting temperature as determined by the Hoffman–Weeks method,[20] V_u represents the molar volume, v_1 stands for the volume fraction of noncrystallizable component in the blend, and X_{23} is the Flory–Huggins thermodynamic interaction parameter. A negative value of the parameter indicates that the blend is compatible, its positive value characterizing the blend as noncompatible.

The graphic representation of the equation applied to our systems can be seen in Figure 7. The slopes of the curves yield the value of X_{23} as compiled in Table II. When the PVF_2/PMMA system incorporated low SEP portions, the interaction parameter was negative. With intermediate SEP portions, the parameter became more and more negative, which is interpreted as an increase in the degree of interaction between the components. The system was then compatible over the whole compositional range under study, SEP content having no influence on compatibility.

For the PVF_2/PS system [Fig. 7(B)] with low SEP content, the interaction parameter was positive and hence the system incompatible. With increasing SEP content in the blend the parameter had increasingly negative values (Table II), which is indicative of the fact that the incompatible PVF_2/PS system was being compatibilized with 10% SEP.

These results are supported by a parallel study with the scanning electron microscope. Figure 8 shows the microphotographs of the PVF_2/PS system (30/70) without SEP incorporation [Fig. 8(A)] and in the presence of 20% SEP [Fig. 8(B)]. In Figure 8(A) the two phases are distinctly visible. In Figure 8(B) phase disappearance is interpreted as an exclusive consequence of the presence of SEP. These observations were identical for the different compositional variants of the system.

Regarding inverse gas chromatography, the fun-

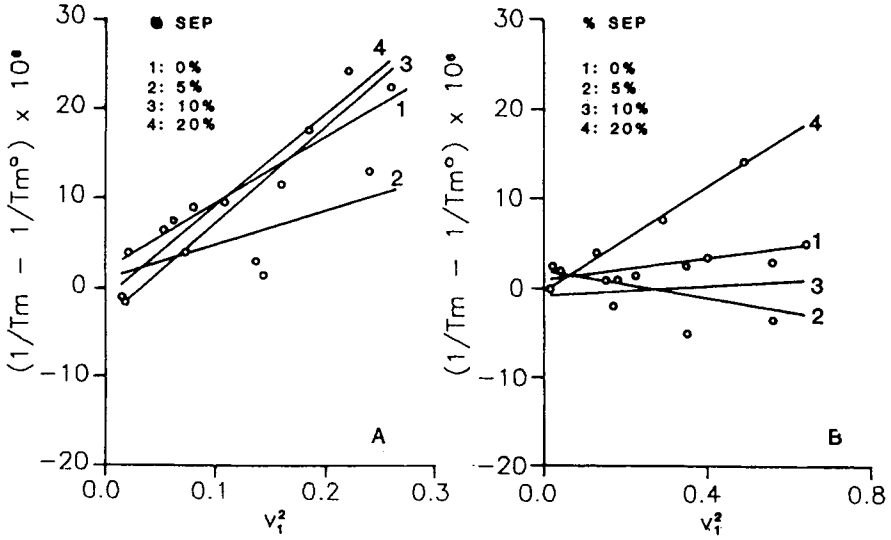

Figure 7 Plot of $(1/T_{m^\circ})$ versus the square of the volume fraction of amorphous polymer (v_1^2) of (A) PVF_2/PMMA and (B) PVF_2/PS blends at different loading of SEP.

damental equation that relates the interaction occurring between a polymer supported by a stationary phase and a solvent was formulated in the following expression, which fundamentally relates the Flory–Huggins interaction parameter X_{12} to the retention volume[22]:

$$X_{12} = \ln\left(\frac{273.16Rv_2}{V_g^\circ P_1^\circ V_1}\right) - \left(\frac{1 - V_1}{M_2 v_2}\right)\phi_2 - \frac{P_1^\circ(B_{11} - V_1)}{RT} \quad (6)$$

where V_g° is the specific retention volume, V_1 the molar volume of the pure (liquid) phase, P_1° is the vapour pressure at temperature T, R represents the gas constant, v_2 the specific volume of the polymer, M_2 stands for molecular weight, and B_{11} identifies the second virial coefficient as obtained from the Dymond–Smith compilations.[22] The vapour pressures of the solute were obtained from Riddick–Bunger's tables,[23] the solute densities were taken from Orwoll–Flory's compilations[24] as well as from Timmermans.[25]

The chromatographic expression of the interaction parameter of a system consisting of a stationary phase resulting from the blend of two polymers was formulated as follows[18]:

$$X_{1(23)} = \ln\left(\frac{273.16R(w_2v_2 + w_3v_3)}{P_1^\circ V_g^\circ V_1}\right) - 2 - \frac{P_1^\circ(B_{11} - V_1)}{RT} = \left[\frac{X_{12}}{V_1}\phi_2 + \frac{X_{13}}{V_1}\phi_3 - \frac{X_{23}}{V_2}\phi_2\phi_3\right]V_1 \quad (7)$$

Table II Interaction Parameters and Intercept of Different PVF_2/PMMA and PVF_2/PS Systems at 433 K

System	X_{23} (cal/cm³)	Intercept 10^6
PVF_2/PMMA (0% SEP)	−0.139	2.87
PVF_2/PMMA (5% SEP)	−0.071	6.82
PVF_2/PMMA (10% SEP)	−0.202	8.37
PVF_2/PMMA (20% SEP)	−0.192	11.09
PVF_2/PS (0% SEP)	0.013	0.68
PVF_2/PS (5% SEP)	0.017	6.48
PVF_2/PS (10% SEP)	−0.006	7.60
PVF_2/PS (20% SEP)	−0.064	12.83

Table III Polymer Solvent Interaction Parameters X_{12} Obtained From Inverse Gas Chromatography Data

	X_{12}		
Solute	PVF_2	PMMA	PS
Hexane	−1.396	−0.485	−1.709
Heptane	−1.463	−6.197	−2.349
Octane	−0.932	—	−2.686
Dichloromethane	−1.822	−4.451	−1.947
Furane	−2.702	−4.370	0.671

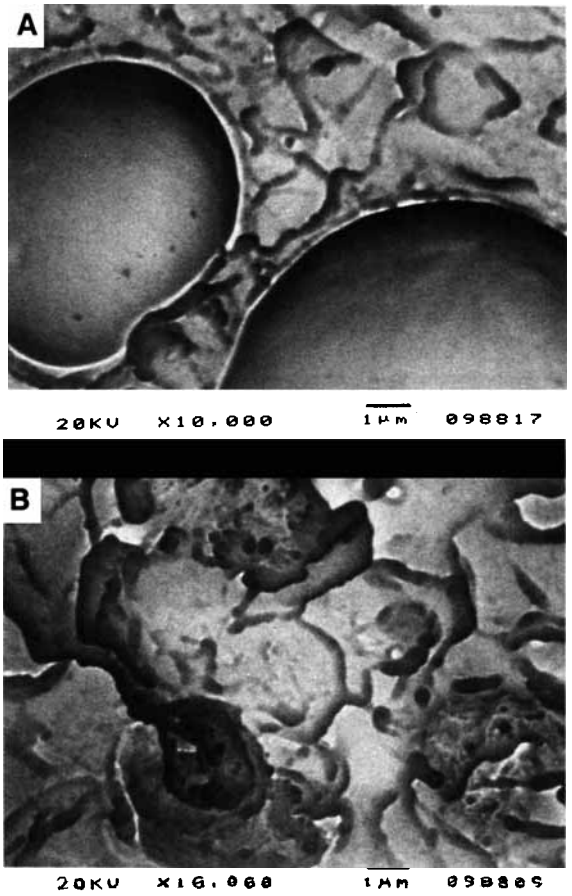

Figure 8 SEM micrographs of the fractured surface of PVF_2/PS 30/70 blend: (A) unfilled and (B) 20 wt % SEP filled.

Table IV Interaction Parameters $X_{1(23)}$ Obtained for PVF_2/PMMA and PVF_2/PS Blends From Inverse Gas Chromatography Data

	$X_{1(23)}$			
	PVF_2/PMMA (wt %)		PVF_2/PS (wt %)	
Solute	70/30	30/70	70/30	30/70
Hexane	−2.924	−2.110	−2.655	−2.559
Heptane	−2.977	−1.871	−2.189	−2.122
Octane	−2.920	−1.476	−2.784	−2.648
Dichloromethane	−2.080	0.850	−2.759	−2.731
Furane	−3.925	10.797	−3.387	−3.532

where w_2 and w_3 are the weight fraction of the blend components, X_{12} and X_{13} are determined from the pure stationary phases.

Table III compiles the values of the polymer–solute interaction parameter (X_{12}) reached by the different polymers. In the case of stationary phases (SEP) supporting PVF_2, X_{12} is always negative reading its highest values with polar solutes.

The values of X_{12} in the case of supports containing PS are slightly higher than the ones computed for PVF_2, except in the case of furane. For PMMA-containing supports the values recorded were higher than those obtained for the other two polymers. The negative values of the interaction pa-

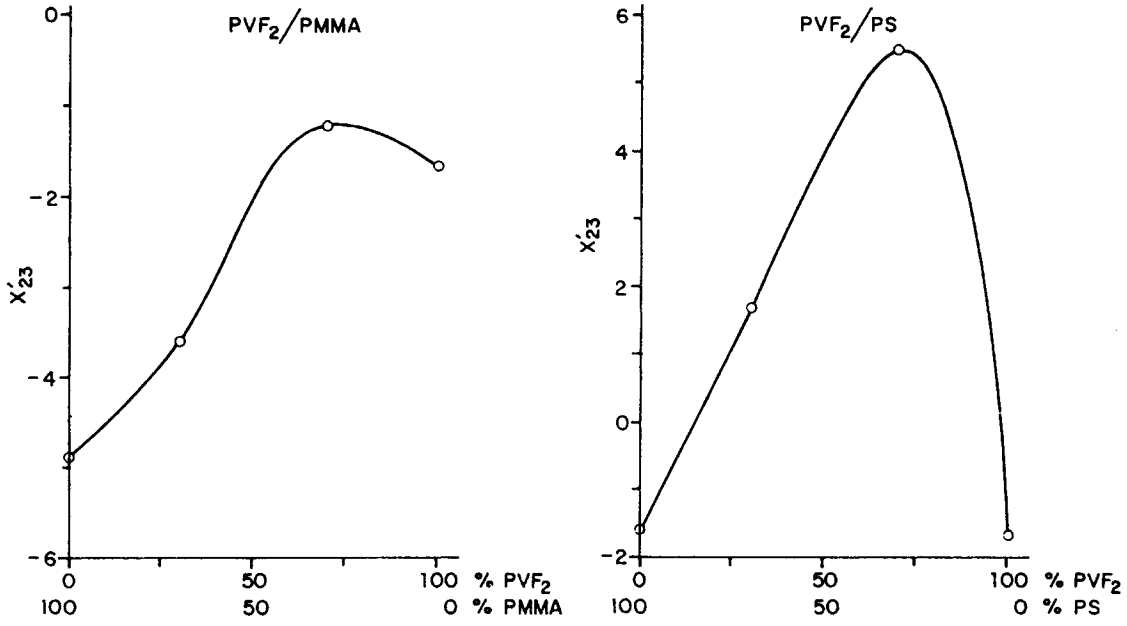

Figure 9 Average polymer–polymer interaction parameter X'_{23} versus blend compc (A) PVF_2/PMMA and (B) PVF_2/PS.

rameter indicate the solubility of the solvent in the polymer.

Table IV shows the values of X_{23} in the case of stationary phases consisting of a polymer blend. The graphic plot of X_{23} against the composition (Fig. 9) shows the PVF_2/PMMA system to be compatible for any blend composition. In the system PVF_2/PS, the interaction parameter values computed were positive, which evidences component incompatibility. At PS concentrations above 85%, however, X_{23} became negative and hence the blend was made compatible.

Hence it is legitimate to conclude that SEP compatibilizes the incompatible PVF_2/PS system, as supported by the interpretation of the data obtained from inverse gas chromatography, melting point depression, and scanning electron microscopy. The criteria, however, that relate the T_g to compatibility did not yield optimum results due to the limitations of the measuring method proper.

The authors acknowledge the financial support received from the Comision Interministerial de Ciencia y Tecnología del Plan Nacional (Spain, Project MAT. 88-0192).

REFERENCES

1. F. J. Gutierrez Monrreal, and C. M. Mari, *Sensors y Actuators,* **12,** 129 (1987).
2. H. S. Nalwa, *Rev. Macromol. Chem. Phys.,* **C31,** 341 (1991).
3. G. Olabisi, L. M. Robenson, and M. T. Shaw, *Polymer-Polymer Miscibility,* Academic Press, 1979.
4. T. Pazonyi and M. Dimitrov, *Rubber Chem. Technol.,* **40,** 1119 (1967).
5. V. N. Koleznev, Yu. S. Maloshchuk, G. I. Grigorya, and B. A. Dogadkin, *Polym. Sci. USSR,* **13,** 62 (1971).
6. N. G. Gaylord, *Chemtechnology* **6,** 392 (1976).
7. N. K. Kalfoglou, *J. Appl. Polym. Sci.,* **32,** 5247 (1986).
8. D. C. McCarthy, Ph.D. thesis, Lehigh University, Lehigh, PA, 1984.
9. W. H. Jo and B. G. Min, *J. Kor. Soc. Textile Eng. Chem.,* **10,** 41 (1986).
10. A. Aref-Azar, J. N. Hay, B. J. Marsden, and N. Walker, *J. Polym. Sci., Polym. Phys. Ed.,* **18,** 637 (1980).
11. M. J. Avrami, *Chem. Phys.,* **7,** 1103 (1939).
12. D. Turnbull and J. C. Fisher, *J. Chem. Phys.,* **17,** 71 (1949).
13. T. Nishi and T. T. Wang, *Macromolecules,* **8,** 909 (1975).
14. L. Mandelkern, *Crystallization of Polymers,* McGraw-Hill, New York, 1964.
15. T. Murayama, *Dynamic Mechanical Analysis of Polimeric Materials,* Elsevier Science Pub., New York, 1978.
16. M. Gordon and J. S. Taylor, *J. Appl. Chem.,* **2,** 493 (1952).
17. T. G. Fox, *Bull. Am. Chem. Soc.,* **1,** 123 (1965).
18. R. L. Scott, *J. Chem. Phys.,* **17,** 279 (1949).
19. R. Konningsveld, L. A. Kleintjens, and R. A. Schultz, *J. Polym. Sci.,* **A2,** 1261 (1970).
20. J. D. Hoffman and J. J. Weeks, *J. Res. Natl. Bur. Stand.,* **A66,** 13 (1962).
21. C. R. Herrero, Ph.D. Thesis, Complutense University, Spain, 1991.
22. J. H. Dymond and E. B. Smith, *The Virial Coefficients of Pure Gases and Mixtures,* Clarendon Press, Oxford, 1980.
23. J. A. Riddick and W. B. Bunger, *Techniques of Chemistry. Organic Solvents,* Vol. II, John Wiley & Sons, Canada, 1970.
24. R. A. Orwoll and P. J. Flory, *J. Am. Chem. Soc.,* **89,** 6814 (1967).
25. J. Timmermans, *Physico-Chemical Constants of Pure Organic Compounds,* Elsevier, New York, Vol. 1, 1950, Vol. 2, 1965.

Received January 26, 1993
Accepted July 7, 1993